IOP Publishing Superconductor Science and Technology
Supercond. Sci. Technol. 31 (2018) 015021 (11pp) https://doi.org/10.1088/1361-6668/aa9b09

Towards a 20 kA high temperature superconductor current lead module using REBCO tapes

R Heller, N Bagrets, W H Fietz, F Gröner, A Kienzler, C Lange and M J Wolf

Karlsruhe Institute of Technology, Institute for Technical Physics, Karlsruhe, Germany

E-mail: reinhard.heller@kit.edu

Received 10 October 2017, revised 7 November 2017
Accepted for publication 16 November 2017
Published 13 December 2017

Abstract

Most of the large fusion devices presently under construction or in operation consisting of superconducting magnets like EAST, Wendelstein 7-X (W7-X), JT-60SA, and ITER, use high temperature superconductor (HTS) current leads (CL) to reduce the cryogenic load and operational cost. In all cases, the 1st generation HTS material Bi-2223 is used which is embedded in a low-conductivity matrix of AgAu. In the meantime, industry worldwide concentrates on the production of the 2nd generation HTS REBCO material because of the better field performance in particular at higher temperature. As the new material can only be produced in a multilayer thin-film structure rather than as a multi-filamentary tape, the technology developed for Bi-2223-based current leads cannot be transferred directly to REBCO. Therefore, several laboratories are presently investigating the design of high current HTS current leads made of REBCO. Karlsruhe Institute of Technology is developing a 20 kA HTS current lead using brass-stabilized REBCO tapes—as a further development to the Bi-2223 design used in the JT-60SA current leads. The same copper heat exchanger module as in the 20 kA JT-60SA current lead will be used for simplicity, which will allow a comparison of the newly developed REBCO CL with the earlier produced and investigated CL for JT-60SA. The present paper discusses the design and accompanying test of single tape and stack REBCO mock-ups. Finally, the fabrication of the HTS module using REBCO stacks is described.

Keywords: current lead, high temperature superconductor, REBCO, fusion magnets

(Some figures may appear in colour only in the online journal)

1. Introduction and objectives

High temperature superconductor (HTS) current leads (CL) in the range of 10–80 kA under fabrication or in operation worldwide, exclusively use Bi-2223 multi-filamentary material (so-called 1st generation HTS) embedded in an AgAu matrix. Examples for machines using HTS CL are the LHC accelerator at CERN and the fusion devices W7-X, JT-60SA, and ITER. The Karlsruhe Institute of Technology KIT constructed the 68 kA ITER demonstrator using Bi-2223 stacks fabricated by American Superconductor which was operated even at 80 kA with He- and at 68 kA with LN2-cooling [1, 2]. The HTS CL for W7-X and JT-60SA, also constructed by KIT, contain Bi-2223 stacks made by Bruker. More details can be found in [3].

In the meantime, HTS manufacturers worldwide concentrate on the production of the 2nd generation HTS REBCO material. This material has superior superconducting properties for the application e.g. in magnets, generators, and motors that causes industry to focus on this material.

Regarding the future use of HTS in CLs, it is mandatory to demonstrate the applicability of the industrially favored REBCO material. Several laboratories are presently investigating the design of a high current HTS connector/current lead made with REBCO [4–6]. KIT has recently finished the manufacturing of the HTS current leads for the supply of the

TF and CS/PF coils of the satellite tokamak JT-60SA [7]. The aim of the new development is the design and construction of a 20 kA HTS current lead where the HTS part is made of REBCO material. In contrast to the previously used multi-filamentary flat Bi-2223 tapes, REBCO tapes are fabricated by depositing the superconducting layer on insulating buffer layers and a highly resistive Hastelloy or Nickel–Tungsten substrate tape. Thus, the current transfer to the superconducting layer can only be performed from the top side and consequently, the design for current transfer to the superconductor realized in the presently used Bi-2223 CL cannot be used. To allow an easy comparison of the REBCO CL, the layout of the 20 kA JT-60SA CL has been used, i.e. only the HTS module was changed from Bi-2223 to REBCO.

To achieve a compact design and to match the available space, the REBCO tapes cannot be arranged next to each other in a single layer along the perimeter of the CL. Thus, the tapes have to be grouped in a number of stacks arranged on the outer surface of a cylindrical structure, as it was done for the Bi-2223 CLs. A direct consequence of this geometrical structure is that the stacks need a staircase arrangement at both ends to be able to transfer the current from the copper end caps at the heat exchanger and the cold end part to each REBCO tape individually.

The material used for electrical stabilization of the tape in case of a quench has to be carefully selected to keep the heat loads within the design specifications. As outcome of material investigations [8], brass-stabilized REBCO tapes are chosen for use in the 20 kA REBCO module. In particular, the brass tape has to be connected to the side of the superconducting layer of the tape.

A consequence of the highly resistive barrier caused by the buffer and substrate, a possible current redistribution can only be achieved via these ends. Therefore, a good thermal contact between the tapes, the stabilizer, and the structure is mandatory.

2. General design of the 20 kA REBCO current lead

The design of the 20 kA REBCO current lead is adopted from the JT-60SA PF current leads and consists of

- a resistive copper heat exchanger HX of meander flow type including the room temperature connection. It covers the temperature range from room temperature to 60 K and is actively cooled by 50 K helium gas,
- an HTS module covering the temperature range from 60 to 4.5 K cooled by heat conduction from the low temperature end where REBCO HTS tapes are used,
- a low temperature connection to the superconducting feeder at 4.5 K equipped with a Nb_3Sn insert to reduce the resistive losses.

Table 1 summarizes the main specifications of the REBCO current lead.

The main tasks of this development are the selection of the REBCO tape including the stabilizer material in order to get a heat load in the 20 kA CL comparable to the JT-60SA CL and the optimization of the soldering process required to achieve a low electrical resistance and a good current transfer from the copper end caps of the HTS module to the tapes.

3. Characterization of selected REBCO tapes

To minimize the manufacturing effort, each basic element of the REBCO module is made from 12 mm wide tapes. Two different REBCO tapes were selected as potential candidates for the use in the 20 kA HTS module:

- Non-stabilized tape produced by Superpower (SP),
- SuperOx (SO) tape stabilized with 2 μm of copper per side.

The following parameters are important for the design of the 20 kA HTS module:

- the critical current as a function of the magnetic field and the temperature which is needed to determine the number of tapes to fulfill the required temperature margin, and
- the thermal conductivity along the tape as a function of temperature which is required for the determination of the heat load to the 4.5 K level.

Both tapes were characterized at KIT. Different samples of SP and SO tapes were prepared and photomicrographs were taken to measure the thicknesses of the constituting layers [9]. Table 2 summarizes the main results for SP and SO tapes.

The critical current I_c and its angular dependence was measured at different applied magnetic fields for 77 K and 65 K [10]. Figure 1 shows $I_c(B)$ at 77 and 65 K for magnetic field parallel and perpendicular to the REBCO ab-plane i.e. the tape surface. While the angular dependence of I_c of the SO tape shows the elliptical dependence as expected for an undoped REBCO tape, I_c of the SP tape is different and it looks even different for two samples (M3 and M4). One can also see that the lift factor for 65 K compared to 77 K is 2.43 for SP tape and 2.03 for SO tape.

The data shown here were used to evaluate the number of tapes required to achieve a current sharing temperature of about 80 K. For this, 96 SP tapes or 72 SO tapes are chosen, which are grouped in 24 stacks located on the outer perimeter of the HTS module. Consequently, four SP tapes or three SO tapes per stack are necessary. The resulting contact length for each tape in the step-connection to the Cu ends is 12.5 mm and 16.6 mm for the SP and SO tapes, respectively.

The results of figure 1 are used to evaluate the critical current as a function of temperature. For this, the magnetic self-field of a 20 kA HTS module was calculated for the four-tape and three-tape stack configuration using the code EFFI [11]. Figure 2 shows the critical current versus temperature for the SO and SP tapes at the previously calculated self-field values.

For both tapes, the thermal conductivity was measured in a Physical Properties Measurement System. Details of the

Table 1. Main specifications of 20 kA REBCO current lead.

Parameter	Unit	Value
Nominal current	kA	20
He inlet temperature for HX, $T_{He,in}$	K	50
Nominal temperature at warm end HTS, $T_{100\%HTS}$	K	60
He mass flow rate for HX cooling at 20 kA	g s^{-1}	1.55
Length of HX	m	1.206
Outer diameter of HX including cladding tube	m	0.126
Length of HTS module incl. Cu ends	m	0.480
Outer diameter of HTS module	m	0.118
Contact length between REBCO and Cu end caps	mm	50
Contact resistance at 60 K/4.5 K	nΩ	15/5
Heat load at 4.5 K and $I = 0$ kA	W	~3
Current sharing temperature	K	~80

Table 2. Main parameters of investigated SP and SO tapes.

Parameter	Superpower	SuperOx
Tape width	12 mm	12 mm
Critical current at 77 K, s.f.	289 A	368 A
Critical current at 65 K, s.f.	701 A	748 A
Thickness of Hastelloy substrate	(49 ± 2) μm	(58 ± 2) μm
Thickness of REBCO layer	~1 μm	~1.5 μm
Total thickness of silver layer	(4.9 ± 0.3) μm	(4.6 ± 1) μm
Total thickness of copper stabilizer	—	(4.6 ± 1) μm
Total thickness of tape	(54.9 ± 2) μm	(68.7 ± 2) μm

measurement technique can be found in [12]. Figure 3 shows the thermal conductivity as a function of temperature for the SP (left) and SO (right) tapes. The contributions of the silver layer in both tapes and of the copper sheath in the SO tape are clearly visible. If taking the layer thickness and the thermal conductivity of the constituents of the SP tape, i.e., Hastelloy [13], REBCO [14], and silver with a rather low residual resistivity ratio RRR of 10 [15], it was not possible to reproduce the measurement results even if considering a variation of the silver layer thickness of ±1 μm, see the dashed line (calculation I) in figure 3 left. The main reason for that might be the porosity of the silver layer which has much lower thermal conductivity than the solid material. As to our knowledge there is no information about the thermal conductivity of the silver cap layer available, we used a different way to evaluate k_{Ag} (calculation II) by subtracting cross section area and k from Hastelloy and REBCO from the cross section area and k of the complete tape, which results in:

$$A_{Ag}k_{Ag}(T) = (A_{hast} + A_{REBCO} + A_{Ag}) * k_{tape}(T) - A_{hast} * k_{hast}(T) - A_{REBCO} * k_{REBCO}(T).$$

The results certainly match the data, see solid line in figure 3 left.

For the SO tape the same calculations were made, i.e., Hastelloy [13], REBCO [14], silver with a rather low RRR of 10 [15], and in addition copper with a rather low RRR of 13 [16]. Again, there was a rather large disagreement with the data even if considering a variation of each the silver and copper layer thicknesses of ±1 μm (which is ±2 μm in total), see dashed line in figure 3 right (calculation III). Using the silver properties obtained for the SP tape from calculation II the agreement is better (solid line, calculation IV).

4. Fabrication and pre-tests of single tape mock-ups

For fabrication of the stacks consisting of REBCO and brass tapes, an appropriate soft solder has to be selected. The use of the non-stabilized SP tape requires an Ag containing solder material with a melting temperature below 200 °C, to avoid degradation of the REBCO layer. Possible candidates are Pb60Sn36Ag4 or In97Ag3. Sn96Ag4 which was applied during the stacking process of the Bi-2223 tapes cannot be used because of its high melting temperature of $T = 221$ °C. In50Sn50 was used for the soldering of Bi-2223 stacks into the HTS module for the W7-X and JT-60SA current leads, but it cannot be used for the stacking process with non-Cu-stabilized tapes from SP due to the lack of silver in the solder, which can lead to a degradation of the superconducting properties of the tape. On the other hand, In50Sn50 can be applied for the SO tape due to the presence of the copper layer around the tape.

Different manufacturing strategies were tested in mock-ups where single brass-stabilized REBCO tapes were connected to a stainless-steel structure with copper end caps. The contact length on each side was 20 mm.

1. Prefabrication of brass laminated non-stabilized REBCO tapes using Pb60Sn36Ag4 or In97Ag3 and subsequent soldering to the structure using In50Sn50 and colophony as flux (sample A and B). For the lamination, 100 μm brass tapes were soldered at both sides of the REBCO tape to avoid bending of the laminated tape after soldering.
2. Prefabrication of brass laminated Cu-stabilized REBCO tapes using Pb60Sn36Ag4 or In97Ag3 and subsequent soldering to the structure using In50Sn50 and colophony as flux (sample C and D). Laminates were prepared like samples A and B.

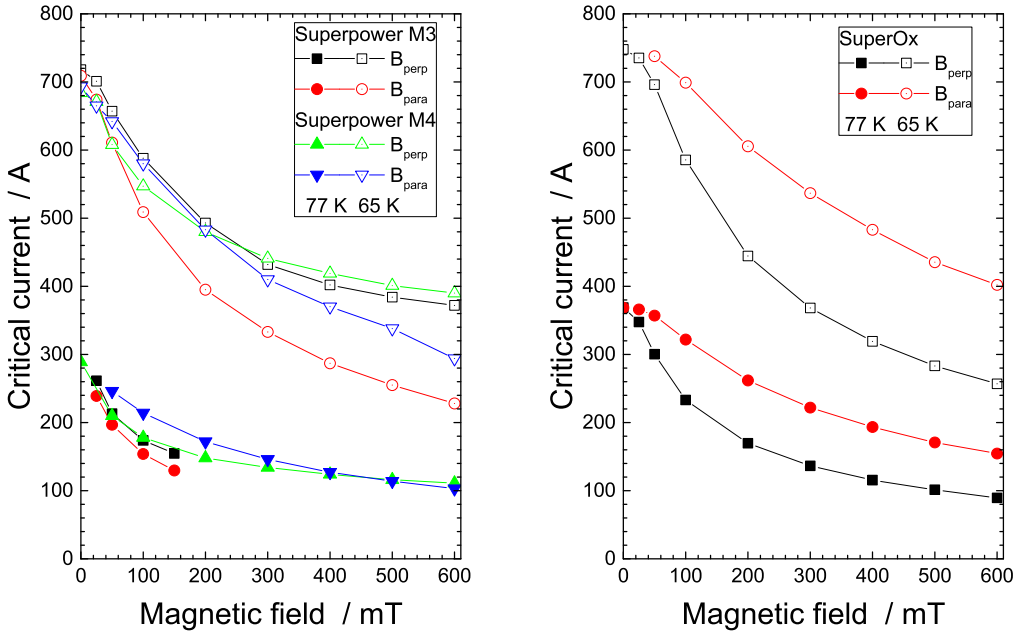

Figure 1. Critical current at 77 K (closed symbols) and 65 K (open symbols) as a function of magnetic field parallel and perpendicular to the *ab*-plane (tape face): SP tapes (left), SO tape (right).

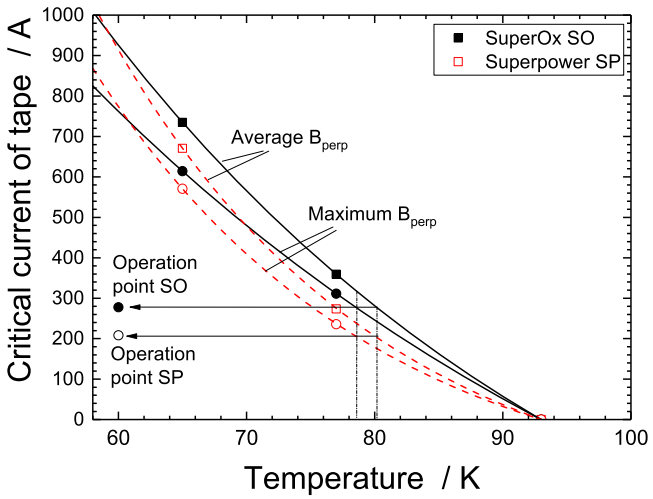

Figure 2. Critical current of single tape at average and maximum magnetic field perpendicular to *ab*-plane as a function of temperature: SP tapes (dashed lines), SO tape (full lines). The resulting operation current is indicated, too.

3. One step soldering of Cu-stabilized REBCO tapes and 300 μm brass tape to the structure using In50Sn50 and colophony as flux (sample E). Here the brass tape was attached to the REBCO tape facing it to the side of the superconductor layer and an additional 100 μm brass tape was put on it from its Hastelloy side for protection.

Figure 4 shows one of the mock-ups prior to soldering of the REBCO tapes.

After fabrication of several samples of type A–E, all mock-ups were tested in a LN_2 bath. The samples were equipped with voltage taps along the tape to measure the contact resistance and the critical current.

A general result of the tests is that the two-step soldering process, i.e., prefabrication of the brass laminated REBCO tape and subsequent soldering in the structure, is not applicable, as the resultant contact resistances are too high and even not reproducible. In some samples the contact resistance was extremely high preventing the determination of the critical current because a significant amount of current was flowing in the stainless steel structure. Only for samples of type D and E acceptable contact resistances were obtained. In particular, for samples of type B non-reproducible results were found. Post mortem check of the quality of the In50Sn50 solder layer showed only 10%–50% of the surface being moistened. Obviously, the colophony flux was not able to remove the oxide layer of the pre-soldered surface of the laminates. On the other hand, sample E was fabricated three times and reproducible good results were obtained.

Figure 5 shows the critical current averaged over several voltage measurement taps along the sample and the contact resistance averaged over both ends. Here the lowest resistances obtained for samples E-1 to E-3 are clearly visible. Five thermal cycles were performed for sample E-2 as well and no change of the performance was observed.

Consequently, SO tapes which are stabilized by a thin Cu layer are used in the further development together with a one-step soldering process.

5. Three-tape HTS-model mock-up

In the 20 kA HTS module, 24 slots of 12.1 mm width could be arranged on the given perimeter. So, it will consist of twenty-four 12 mm wide stacks with three REBCO tapes per stack. A 1/24 model-sample was fabricated and equipped with a three-step staircase copper contact at both ends. After

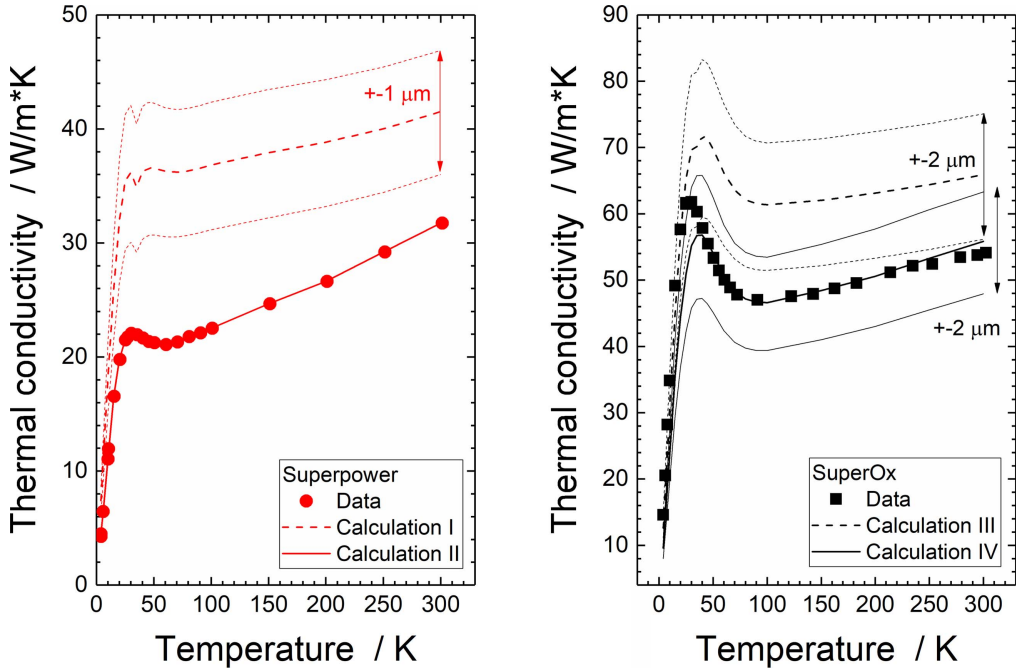

Figure 3. Thermal conductivity of single SP (left) and SO (right) tape. For comparison, the thermal conductivities calculated from solid material are also shown (dashed lines, with a ± 1 μm spread of both the silver and copper layers). Here a large discrepancy is visible. By adjusting the thermal conductivity of silver, one gets a much better agreement (solid lines, with a ± 1 μm spread of each the silver and copper layers).

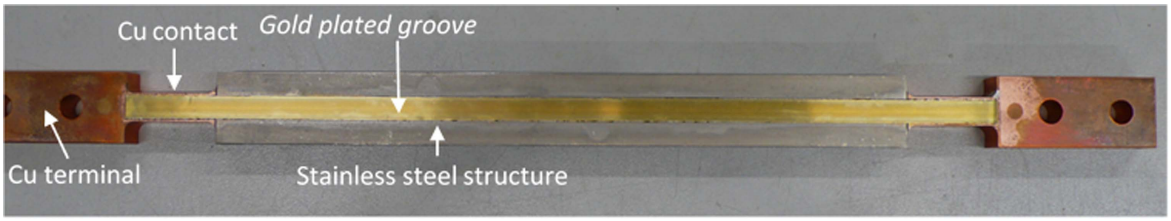

Figure 4. One of the mock-ups prior to soldering. The copper terminals are shown at left and right and the gold plated groove is visible as well.

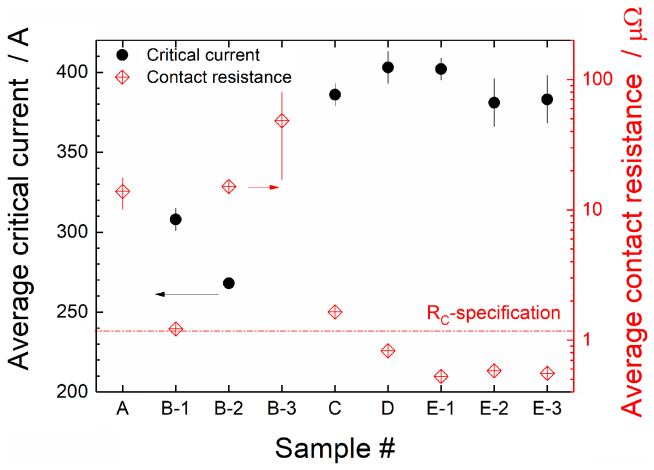

Figure 5. Critical current averaged over several voltage measurement taps along the sample and the contact resistance averaged over both ends for various samples. For samples A and B-3 no critical current could be determined. The specified contact resistance R_C is also indicated as dash-dotted line.

gold plating of the surface, a series of brass and REBCO tapes were arranged in the grooves with intermediate colophony flux and In50Sn50 solder. Then the sample was heated to perform the soldering in a single process. In a next step, the mock-up was tested in LN_2 in the same way as the single tape mock-ups including five thermal cycles.

Figure 6 left shows the voltage in the center of the sample. Current sharing started at approx. 720 A (0.1 μV cm^{-1} criterion) but a power law fit $\left(\frac{E}{E_C}\right) = \left(\frac{I}{I_C}\right)^n$ with $E_C = 1\,\mu$V cm^{-1} for center voltages $>10\,\mu$V results in a critical current of $I_C = 1033$ A and an n-value of $n = 24$. The bump in the voltage trace is due to the fact that the outermost tape carries more current than the central one and the bottom tape carries the lowest current due to non-equal current paths in the copper blocks. Figure 6 right shows the voltage at both contacts as a function of current. The contact resistance was 0.305 $\mu\Omega$ for each end corresponding to $R * A = 1.83\,\mu\Omega\,\text{cm}^2$ for a total contact area of 6 cm^2. This is about a factor of 25 larger than that achieved for copper stabilized REBCO joints [17]. This

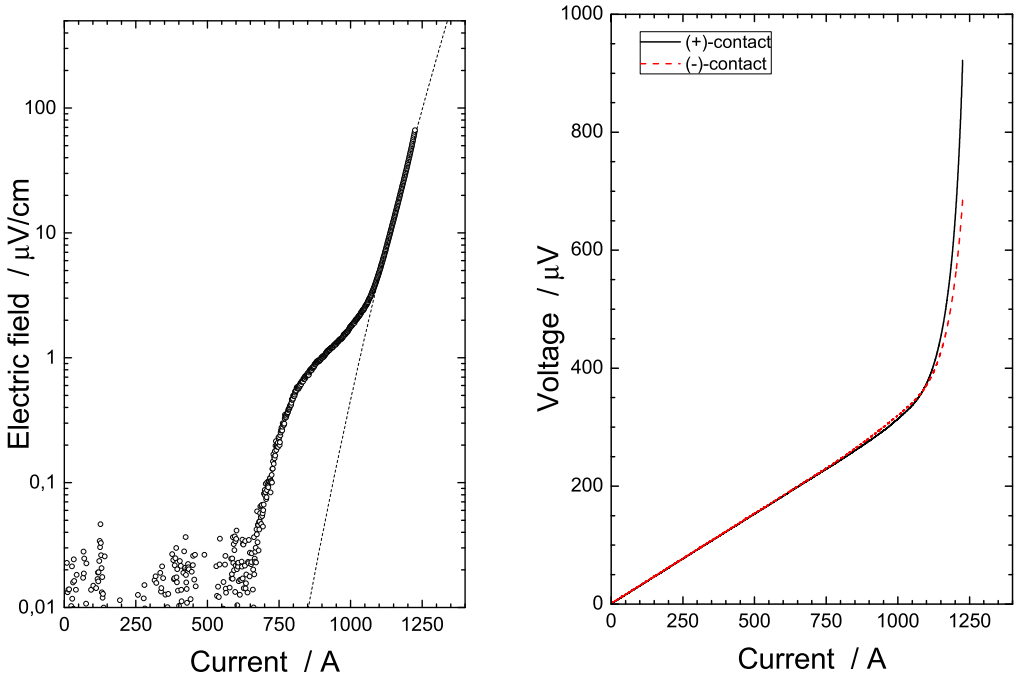

Figure 6. Left: electric field in the center of the sample as a function of current (open circles) and power-law fit (dashed line). Right: voltage at both contacts as a function of current.

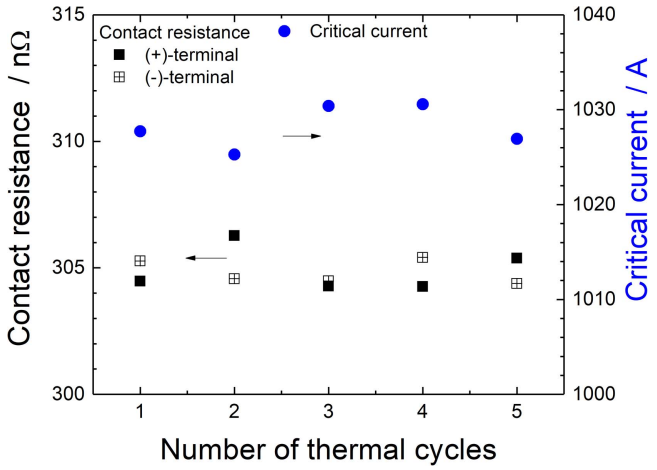

Figure 7. Contact resistance at both ends and critical current averaged over several voltage measurement taps along the sample as a function of the number of thermal cycles.

can be at least partially explained by the contribution of the 300 μm thick brass layer, an additional solder interface layer and part of the copper terminal are included in the contact resistance measurement.

Five thermal cycles were performed for the three-tape sample and the critical current and the contact resistance were measured during each cycle. Figure 7 shows the contact resistance at both ends and the critical current averaged along the sample length as a function of the number of thermal cycles. No change in performance was observed.

A 2-dim electrical model of the mock-up was simulated using the FEMM software [18]. A 2-dim model is suitable because practically no current flows in the thin copper sheath on both sides of the tape [19]. For symmetry reason only one-half of the mock-up was modeled and a thickness of 12 mm was set corresponding to the width of the REBCO and brass tapes. The different thicknesses of the stainless-steel structure (40 mm) and the copper current termination (40 mm) were taken into account by adapting their electrical resistances; this is a reasonable approximation in the 2-dim model. The nominal current of 832 A —corresponding to 1/24 of 20 kA—was imposed at the copper terminal and a constant zero voltage was set as boundary condition at the axial center of the mock-up. Table 3 summarizes the electrical resistivity values of the various components [12–14]; the silver and copper layer of the SO tape were combined with the REBCO layer and a sufficiently low electrical resistivity has been chosen. To match the measured resistivity data, the constant contact resistivity of the various In50Sn50 solder layers had to be adjusted to 1.83 $\mu\Omega$ m—which is more than a factor of 20 larger than the resistivity of the solid solder. By integrating the current density across the tape cross section, a current of 378 A, 249 A,

Table 3. Electrical resistivity of the materials used in the three-tape HTS-model mock-up.

Material	Electrical resistivity at 77 K (Ωm)
Copper of contact part (RRR = 30)	2.54×10^{-9}
Copper of terminal (RRR = 30), corrected for different thickness	7.62×10^{-10}
Stainless steel structure, corrected for different thickness	1.59×10^{-7}
REBCO + silver + copper layers	1.0×10^{-15}
Hastelloy substrate	1.236×10^{-6}
Brass (Cu70Zn30) stabilizer	4.96×10^{-8}
In50Sn50 solder	9.2×10^{-8}
Effective solder layer	1.83×10^{-6}

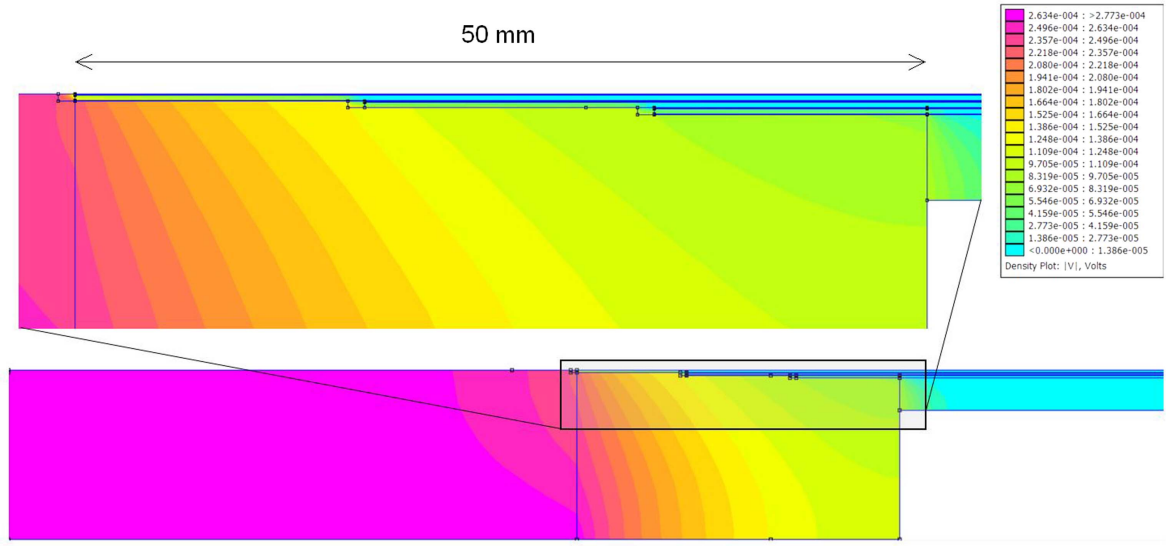

Figure 8. 2-dim model of the voltage distribution in the contact region.

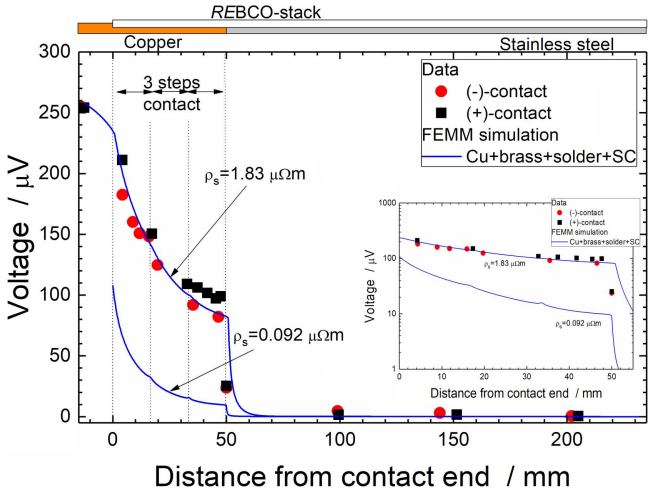

Figure 9. Voltage along both contacts at 832 A measured against the axial center of the sample. The solid lines are the results of simulations using FEMM for resistivity values of the solid solder of 1.83 and 0.092 $\mu\Omega$ m. The inset plot shows an enlargement of the contact area.

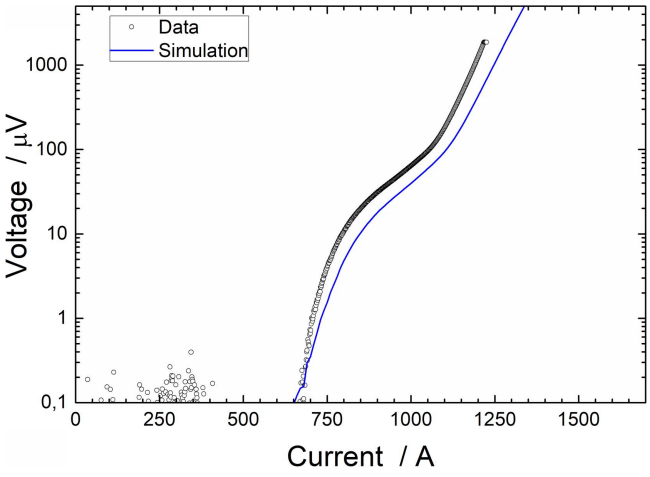

Figure 10. Total voltage along the sample including copper ends with the linear dependence subtracted (open circles). The full line corresponds to results of a simulation of a three-tape parallel circuit.

and 189 A are flowing in the top, center and bottom tape, respectively which is caused by the different resistances of the current flow paths. In addition, about 12 A are flowing to the steel structure and about 4 A to the bottom brass layer. Obviously, the critical current in the top tape is exceeded and current sharing should start already at about 770 A (see figure 9). Figure 8 shows the 2-dim voltage distribution in the contact region.

In figure 9 the measured voltages along both contacts are plotted against the distance from the contact end. Here the three-step geometry in the copper contact region and the sharp voltage drop at the copper-stainless steel interface is clearly visible. For comparison, the results of 2-dim simulations with FEMM for two different resistivity values of the solid solder are also shown as solid lines:

- 1.83 $\mu\Omega$ m (fairly reproducing the data), and
- 0.092 $\mu\Omega$ m (value for solid In50Sn50 solder).

From the contact geometry, we calculated a total contact resistance of 1.69 $\mu\Omega\,\mathrm{cm}^2$ for a resistivity value of the solder of 1.83 $\mu\Omega$ m which is in fair agreement to the measured contact resistance of 1.83 $\mu\Omega\,\mathrm{cm}^2$. Using a solder resistivity of 0.092 $\mu\Omega$ m, the estimated contact resistance is 0.78 $\mu\Omega\,\mathrm{cm}^2$, i.e. a factor of 2.3 lower.

To estimate the contributions of the solder layer, of the brass layer and of the copper terminal, three further simulations were performed leading to resistances of the copper terminal, the brass layer and the (adjusted) solder layers are 0.014, 0.103, and 0.164 $\mu\Omega$.

The effect of the unequal current distribution caused by the different current paths in the copper termination to the three tapes was studied under the assumption that the tapes are only connected at the terminals. This allows modeling them as parallel circuit as suggested in [20]. Thus, the voltage drops U_i ($i = 1, 3$) have to be equal along all tapes and that the sum of all tape currents I_i has to match the total current. The voltage drop U_i on the ith REBCO tape is assumed to

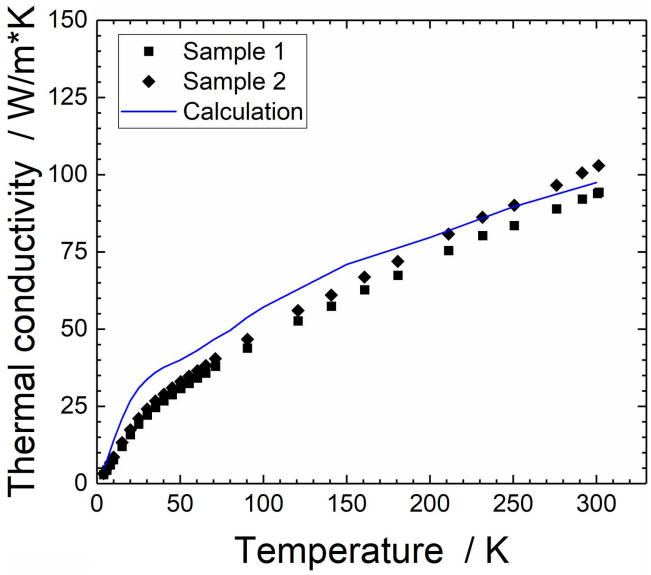

Figure 11. Thermal conductivity along the stack versus temperature of three 3-tape stack samples. The calculated thermal conductivity is also shown as solid line.

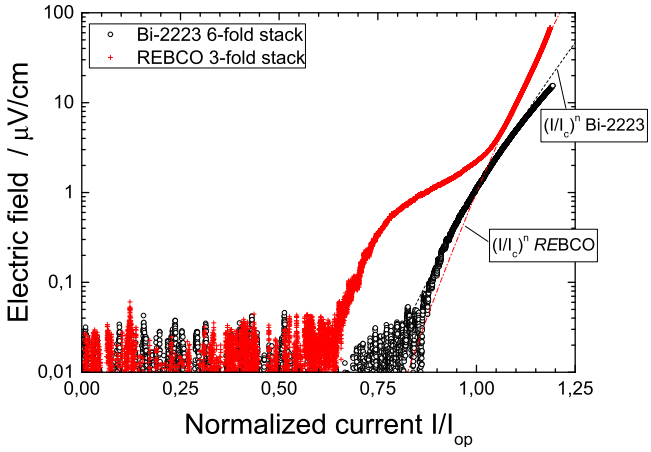

Figure 12. Comparison of the electric field as a function of the normalized current for the 3-tape REBCO and the 6-tape Bi-2223 samples. The power-law fits for the Bi-2223 and REBCO stack are also shown as dashed and dash-dotted lines.

consist of the voltage drop due to the contact resistance R_c, $i * I_i$ and the nonlinear voltage drop in the superconductor $U_c\left(\frac{I}{I_c}\right)^n$. The resulting nonlinear system is solved numerically [21] with the same critical current of 348 A and n-value of 23 for all three tapes and contact resistances of 1.3, 1.0, and 0.64 $\mu\Omega$ for the three tapes. Figure 10 shows the total voltage along the sample including the copper ends with the linear dependence subtracted (open circles). The modeled voltage–current trace is shown as a full line and represents well the measured voltage–current characteristics.

A three-tape stack was fabricated and longitudinally cut in three samples of the same width for measuring the thermal conductivity along the stack. Figure 11 shows the thermal conductivity as a function of temperature for two three-fold stack samples. The main contribution to the thermal conductivity is the brass stabilizer.

Integration of the thermal conductivity between 4 and 60 K gives 1205 and 1307 W m^{-1} for the two samples. The Bi-2223/AgAu stack—as a reference—has an integral thermal conductivity of 1480 W m^{-1}.

6. Comparison of REBCO and Bi-2223 stacks

As a reference, one sample mock-up was fabricated using a 4 mm wide six-tape Bi-2223 stack of the same production batch as used for the HTS current leads W7-X [22] and JT-60SA. The sample was then tested in LN_2 in the same way as the REBCO sample. Figure 12 shows a comparison between the electric field–current traces of both samples:

- To visualize the electric field–current dependency, the current was normalized to the critical current (i.e., $I_c = 467$ A and $n = 17$ for the Bi-2223 stack and $I_c = 1033$ A and $n = 24$ for the REBCO-stack) to achieve a comparable result. For the REBCO sample, current redistribution starts at $I/I_c \approx 0.65$ (i.e. $I = 671$ A) and at 1090 A—which corresponds to 4 μV cm^{-1}—the quench of the whole stack develops. For an electric field of 1 μV cm^{-1}, the REBCO stack is in the current redistribution regime. In case of the Bi-2223 sample, current sharing of the whole stack starts at at $I/I_c \approx 0.75$ (i.e. $I = 350$ A) and beyond 400 A the normal zone propagation develops reaching $I_c = 467$ A for $\Delta U/\Delta l = 1$ μV cm^{-1}. The marginal convex curvature indicates a slight current redistribution due to the unequal magnetic field at the individual tapes of the six-fold Bi-2223 stack. It should be noted that the voltage measured along the whole stack excluding the copper terminals results in a critical current of 468 A which is close to the value measured by the manufacturer in 2012 ($I_c = 470$ A).
- Regarding the contact resistance, the result for the Bi-2223 stack is 0.3035 $\mu\Omega$ or 0.3642 $\mu\Omega$ cm^2, which is a factor of five smaller than that for the REBCO stack (1.83 $\mu\Omega$ cm^2). The resultant expected contact resistances of a 20 kA HTS module are 12.8 nΩ (REBCO) and 5.1 nΩ (Bi-2223) both at 77 K.

7. Description of the 20 kA REBCO-module

7.1. General

The base of a 20 kA REBCO-module consists of a stainless-steel tube with brazed copper end caps on each end. In this base, slots were milled to host the three brass/REBCO tapes units per slot with the stepwise current transfer region on each Cu end. The 72 SO tapes needed for the 20 kA module, are grouped in 24 stacks with three tapes per stack. Before soldering the brass and REBCO tapes to the module, all contact surfaces of the module were gold plated to prepare them for soldering. Figure 13 shows a picture of the module prior to

Figure 13. Picture of the 20 kA REBCO-module prior to gold plating. The grooves with the staircase like end at the copper end caps are clearly visible.

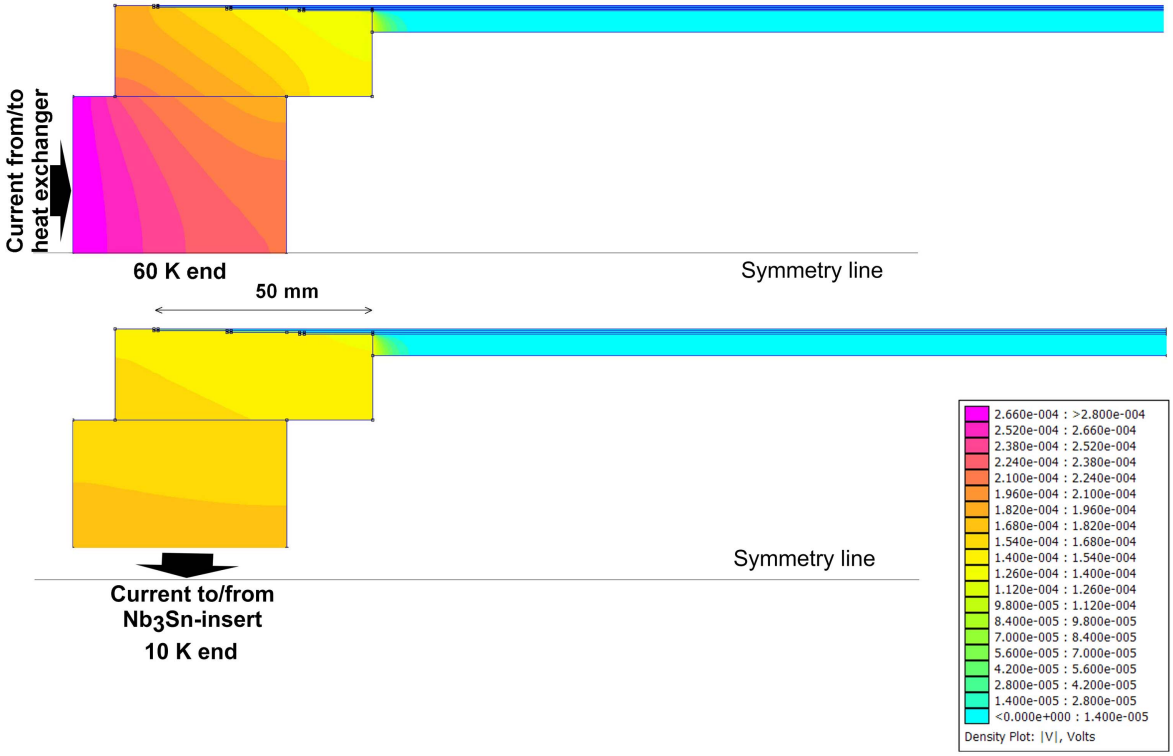

Figure 14. 2-dim model of the voltage distribution of the upper (top) and lower (bottom) half of the module.

Table 4. Electrical resistivity of the materials used in the HTS module.

Material	Electrical resistivity at 60 K (Ωm)	Electrical resistivity at 10 K (Ωm)
Copper of contact part (RRR = 50)	1.29×10^{-9}	3.15×10^{-10}
Stainless steel structure	5.10×10^{-7}	4.90×10^{-7}
REBCO + silver + copper layers	1.0×10^{-15}	1.0×10^{-15}
Hastelloy substrate	1.234×10^{-6}	1.230×10^{-6}
Brass (Cu70Zn30) stabilizer	4.50×10^{-8}	4.22×10^{-8}
Effective solder layer	1.83×10^{-6}	1.83×10^{-6}

gold plating. The grooves with the staircase like end at the copper end caps are clearly visible.

7.2. Contact resistance and critical current

A FEMM model of 1/24 of the HTS module was built and the voltage distribution and resultant resistances were computed for the 60 and 10 K ends. Table 4 summarizes the electrical resistivity of the materials used in the model. While the solid materials have a temperature dependent resistivity it is assumed that the effective solder layer does not. Figure 14 shows the 2-dim model of the voltage distribution of the upper (top) and lower (bottom) half of the module. The resultant contact resistances at 60 and 10 K are 0.337 and

Table 5. Comparison of Bi-2223 and REBCO 20 kA current leads designs.

Parameter	20 kA HTS CL (JT-60SA)	20 kA HTS CL (REBCO)
HTS material	Bi-2223/AgAu	REBCO/brass
Maximum current	20 kA	
Heat load at 4.5 K end for 0 kA	2.82 W	2.16 W
He mass flow rate at 0 kA	0.402 g s^{-1}	0.407 g s^{-1}
He mass flow rate at 20 kA	1.560 g s^{-1}	1.572 g s^{-1}

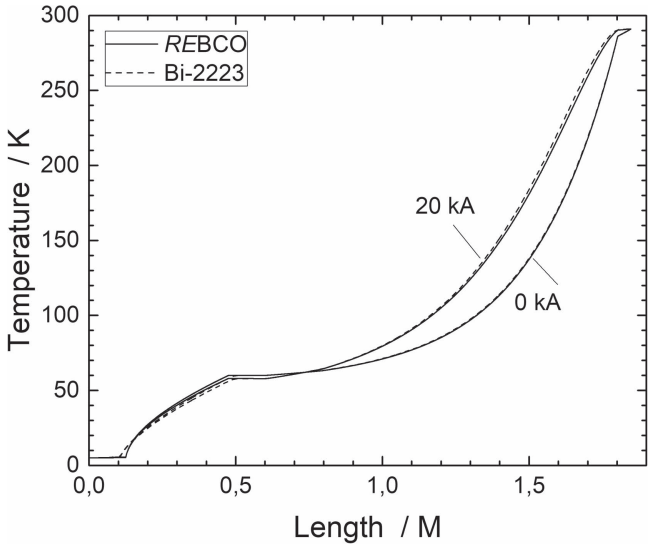

Figure 15. Temperature profiles of the 20 kA REBCO current lead for 0 and 20 kA (solid lines) and comparison to the Bi-2223 current lead.

0.208 $\mu\Omega$ from which the contact resistances of the HTS module of 14.05 and 8.66 nΩ are calculated. Here the copper terminals are included. Furthermore, the model also gives the currents in the individual tapes by integrating the current density across the tape cross section. The result is 243 A in the bottom tape, 277 A in the center tape and 314 A in the top tape.

7.3. Prediction of the 20 kA REBCO current lead performance

The computer code CURLEAD [23] was used during the design of the 20 kA REBCO current lead. For this the thermal conductivity as measured for the three-fold stack (see figure 11) has been taken as material input. The results were compared to those obtained for the 20 kA Bi-2223 current lead as manufactured for JT-60SA [24]. Figure 15 shows the temperature profiles of the 20 kA REBCO current lead for 0 and 20 kA (solid lines) and comparison to the Bi-2223 current lead (dashed lines). The temperature profiles along the REBCO and JT-60SA current leads are almost identical, with small deviations in the HTS-module region, which is caused by the different lengths of the Cu ends of the module. Table 5 summarizes the main results of the design calculations. The difference in the heat load at the 4.5 K end is caused by the different thermal conductivity of the stacks. The marginal difference in the He mass flow rate is due to the different transition resistances for the REBCO and Bi-2223 CL assumed in the CURLEAD model.

8. Conclusions and outlook

KIT is developing a 20 kA HTS current lead using REBCO material. The aim is to manufacture a current lead from the JT-60SA type but to make the technology available for a 20 kA REBCO module that can replace the Bi-2223 module with a similar performance. Single tape mock-ups were fabricated to optimize the soldering process to achieve a good electrical contact which is a prerequisite for a good current transfer from copper to the superconducting tapes. A one step soldering process using In50Sn50 solder was finally identified to be applied for the fabrication of the 20 kA HTS module.

In a next step, a three-fold stack was fabricated and tested at LN_2 temperature, demonstrating the good performance expected from the single tape mock-up. A comparison to a single six-fold Bi-2223 stack showed that the current transfer in the staircase contact region is influenced by the non-equal current paths.

At present, the 20 kA REBCO current lead has been manufactured and will soon be tested in the current lead test facility CuLTKa [25] at KIT.

Acknowledgments

The authors appreciate the effort of the main workshop of KIT and the current lead assembly crew in ITEP. The work of A Kario and B Ringsdorf who performed the critical current measurements and of K Altmann who investigated the micrographics of the REBCO tapes is acknowledged. This work is financially supported by the German Ministry of Research and Education under the grant No. 03FUS0019. The views and opinions expressed herein do not reflect necessarily those of the BMBF.

ORCID iDs

R Heller https://orcid.org/0000-0002-6600-1861
N Bagrets https://orcid.org/0000-0003-0323-4972

References

[1] Heller R *et al* 2005 Experimental results of a 70 kA high temperature superconductor current lead demonstrator for the ITER magnet system *IEEE Trans. Appl. Supercond.* **15** 1496–9

[2] Heller R, Fietz W H, Lietzow R, Tanna V L, Zahn G, Wesche R and Vostner A 2006 70 kA high temperature superconductor current lead operation at 80 K *IEEE Trans. Appl. Supercond.* **16** 823–6

[3] Heller R, Fietz W H, Kienzler A and Lietzow R 2011 High temperature superconductor current leads for fusion machines *Fusion Eng. Des.* **86** 1422–6

[4] Wesche R, Bykovsky N, Uglietti D, Sedlak K, Stepanov B and Bruzzone P 2016 Commissioning of HTS adapter and heat exchanger for testing of high-current HTS conductors *IEEE Trans. Appl. Supercond.* **26** 9500705

[5] Saggese A, Iannone G, Gambardella U, Califano N and Ferrentino A 2015 20 kA HTS current leads for the INFN magnet test facility *IEEE Trans. Appl. Supercond.* **25** 4801304

[6] Kovalev I A, Surin M I, Naumov A V, Novikov M S, Novikov I, Ilin A A, Polyakov A V, Scherbakov V I and Shutova D I 2017 Test results of 12/18 kA ReBCO coated conductor current leads *Cryogenics* **85** 71–7

[7] Fietz W H, Heller R, Kienzler A and Lietzow R 2009 High temperature superconductor current leads for WENDELSTEIN 7-X and JT-60SA *IEEE Trans. Appl. Supercond.* **19** 2202–5

[8] Drotziger S, Fietz W H, Heller R and Jung A 2016 Investigation of stabilizer material properties used with REBCO coated conductor tapes for the application in a 20 kA high-temperature superconductor current lead *IEEE Trans. Appl. Supercond.* **26** 4801409

[9] Altmann K private communication

[10] Kario A and Ringsdorf B private communication

[11] Sackett S J 1975 Calculation of electromagnetic fields and forces in coil systems of arbitrary geometry *Proc. 6th IEEE Symp. Engineering Problems Fusion Research (San Diego, CA, USA)* pp 935–9

[12] Bagrets N, Barth C and Weiss K P 2014 Low temperature thermal and thermo-mechanical properties of soft solders for superconducting applications *IEEE Trans. Appl. Supercond.* **24** 7800203

[13] Lu J, Choi E S and Zhou H D 2008 Physical properties of Hastelloy C-276 at cryogenic temperatures *J. Appl. Phys.* **103** 064908

[14] Material Database from Cryodata Software Package, CRYOCOMP, version 3.0, Florence, SC, USA, 1997

[15] Material Data base from CryoSoft Software Package, SOLIDS, version 3.5 by CryoSoft, Thoiry, France, 2002

[16] Bonura M and Senatore C 2015 High-field thermal transport properties of REBCO coated conductors *Supercond. Sci. Technol.* **28** 025001

[17] Polak M, Barnes P N and Levin G A 2006 YBCO/Ag boundary resistivity in YBCO tapes with metallic substrates *Supercond. Sci. Technol.* **19** 817–20

[18] Meeker D 2015 *Finite Element Method Magnetics, Version 4.2, User's Manual* http://www.femm.info/Archives/doc/manual42.pdf

[19] Bagrets N, Weiss K P, Nast R and Heller R Correlation between resistances of face-to-face sol-dered joints and interface resistance between layers in superconducting tapes *Presented at EUCAS 2017 Conf.; IEEE Trans. Appl. Supercond.* in preparation

[20] Zermeno V, Krüger P, Takayasu M and Grilli F 2014 Modeling and simulation of termination resistances in superconducting cables *Supercond. Sci. Technol.* **27** 124013

[21] Scilab Enterprises 2012 Scilab: Free and Open Source software for numerical computation (OS, Version 5.5.2) [Software] http://scilab.org

[22] Heller R, Buscher K P, Drotziger S, Fietz W H, Kienzler A, Lietzow R, Mönnich T, Richter T, Rummel T and Urbach E 2013 Status of series production and test of the HTS current leads for Wendelstein 7-X *Fusion Eng. Des.* **88** 1482–5

[23] Heller R 1989 *Numerical Calculation of Current Leads for Fusion Magnets* KfK-4608 Karlsruhe

[24] Heller R, Fietz W H, Heiduk M, Hollik M, Kienzler A, Lange C, Lietzow R, Meyer I and Richter T 2018 Overview of JT-60SA HTS current lead manufacture and testing *IEEE Trans. Appl. Supercond.* **28** 4800105

[25] Richter T, Bobien S, Fietz W H, Heiduk M, Heller R, Hollik M, Lange C, Lietzow R and Rohr P 2017 Design, construction and performance of the current lead test facility CuLTKa *Cryogenics* **86** 22–9